From:
DM+25 (arXiv:2409.09122)
DM+26 (arXiv:2509.02394)
Sersante, **DM**+; in prep.

Extreme mass ratio inspirals: formation and eccentricity

Davide Mancieri

University of Trento and Milano-Bicocca

Collaborators: L. Broggi, M. Bonetti, A. Sesana, B. Sersante, Z. Penoyre, E. M. Rossi, K. L. Muñoz

1st BiCoQ Conference, 18 June 2026

UNIVERSITÀ DEGLI STUDI DI MILANO BICOCCA

UNIVERSITÀ DI TRENTO

Extreme mass ratio inspirals (EMRIs)

Stellar-mass black hole inspiraling into a massive black hole (MBH) of 10^5–10^7 $M_\odot$

Typical mass ratio m/M = 10^{-4}–10^{-6}

colors: different mass ratios

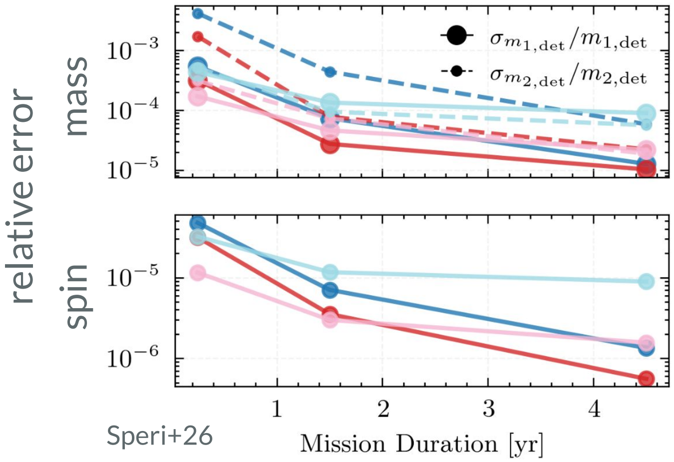

Speri+26

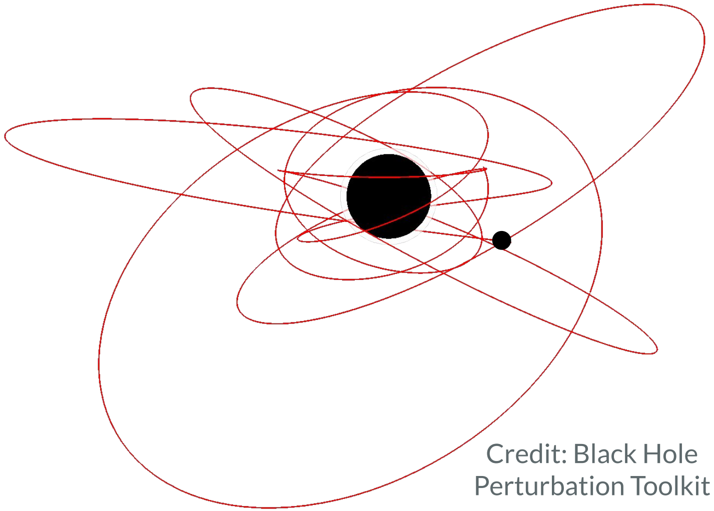

Credit: Black Hole Perturbation Toolkit

LISA sources (mHz): 10–10^3 detections expected

MBH properties measured to 10^{-3}–10^{-6} rel. error and tests of general relativity

EMRI formation via two-body relaxation

nuclear star cluster

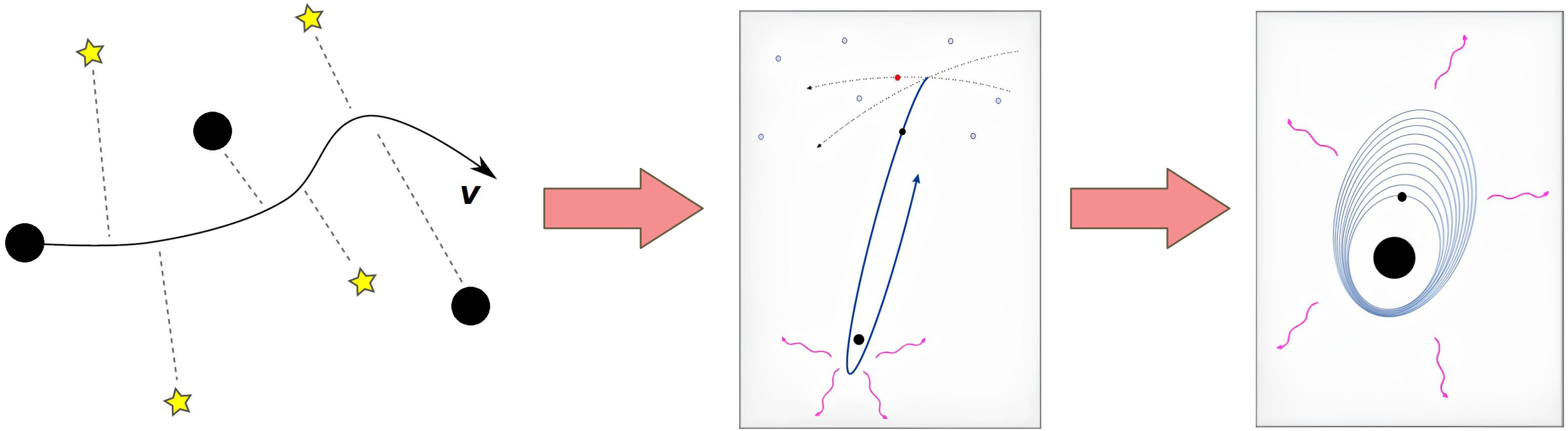

(greatly exaggerated, weak encounters)

Credit: L. Barack

EMRI formation via two-body relaxation

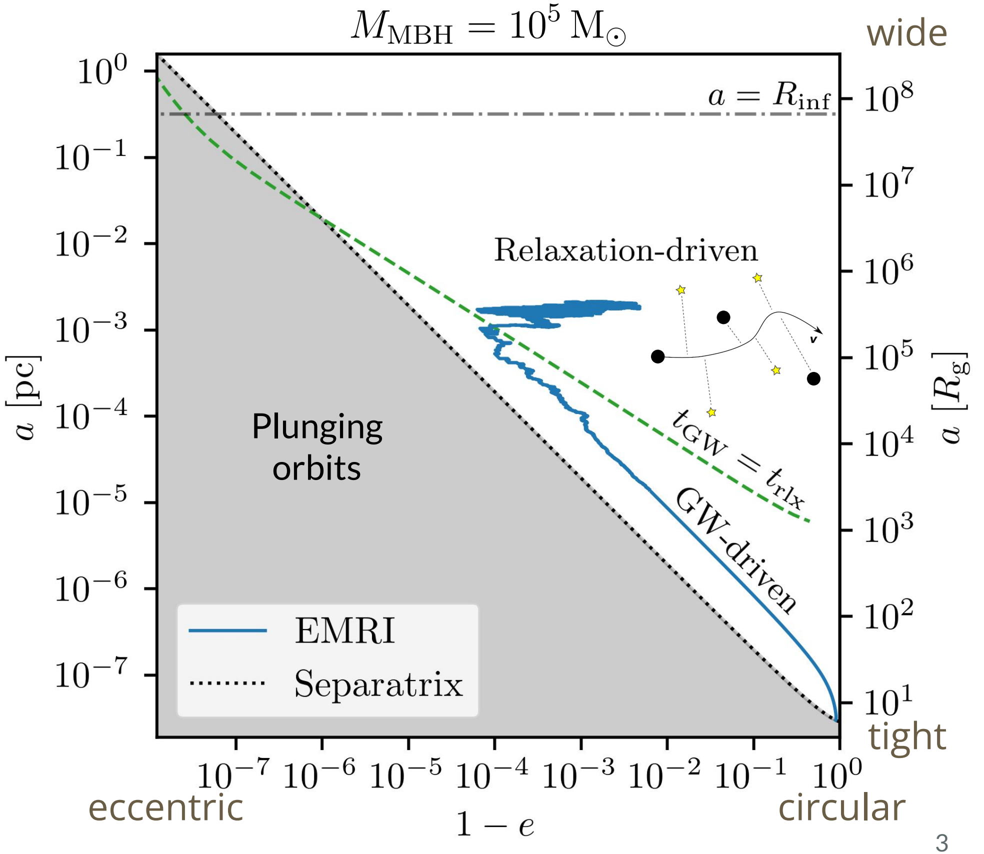

t_{GW} time needed for **GWs** to modify the orbital elements

t_{rlx} time needed for **relaxation** to modify the orbital elements

EMRI formation via two-body relaxation

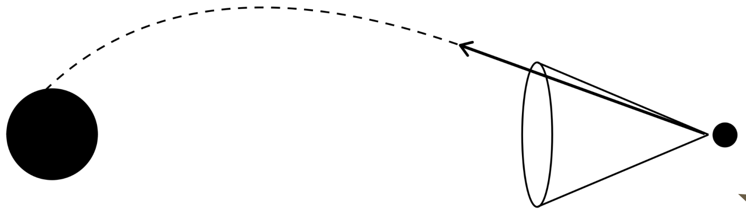

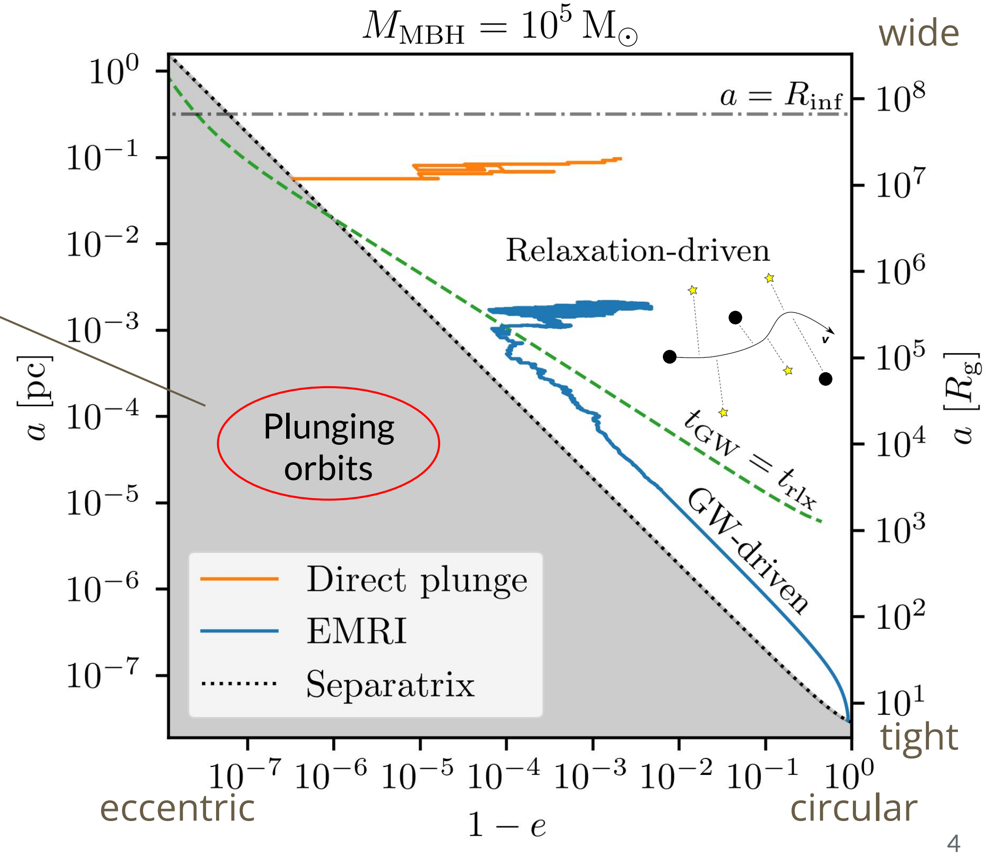

t_{GW} time needed for **GWs** to modify the orbital elements

t_{rlx} time needed for **relaxation** to modify the orbital elements

EMRI formation via two-body relaxation

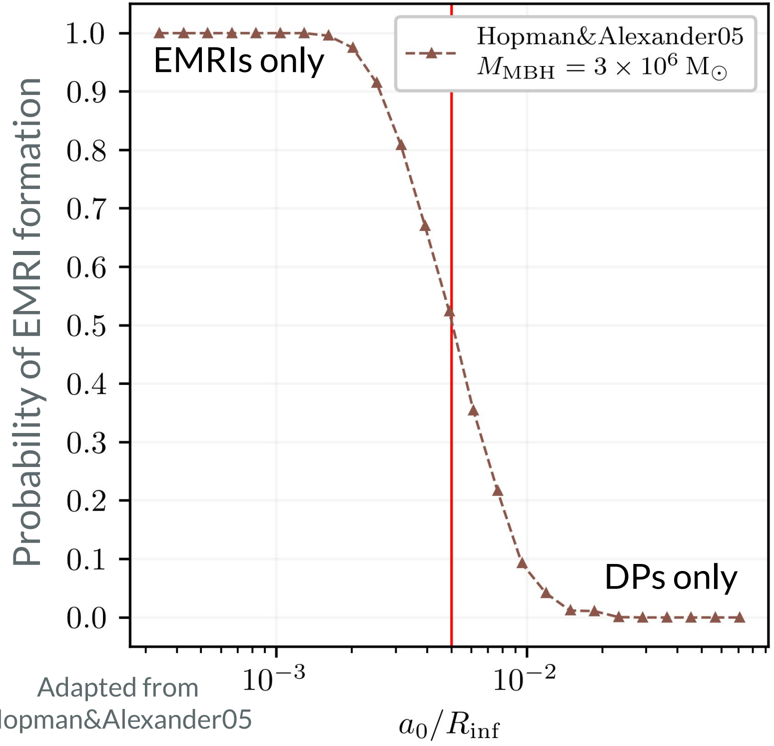

Adapted from Hopman&Alexander05

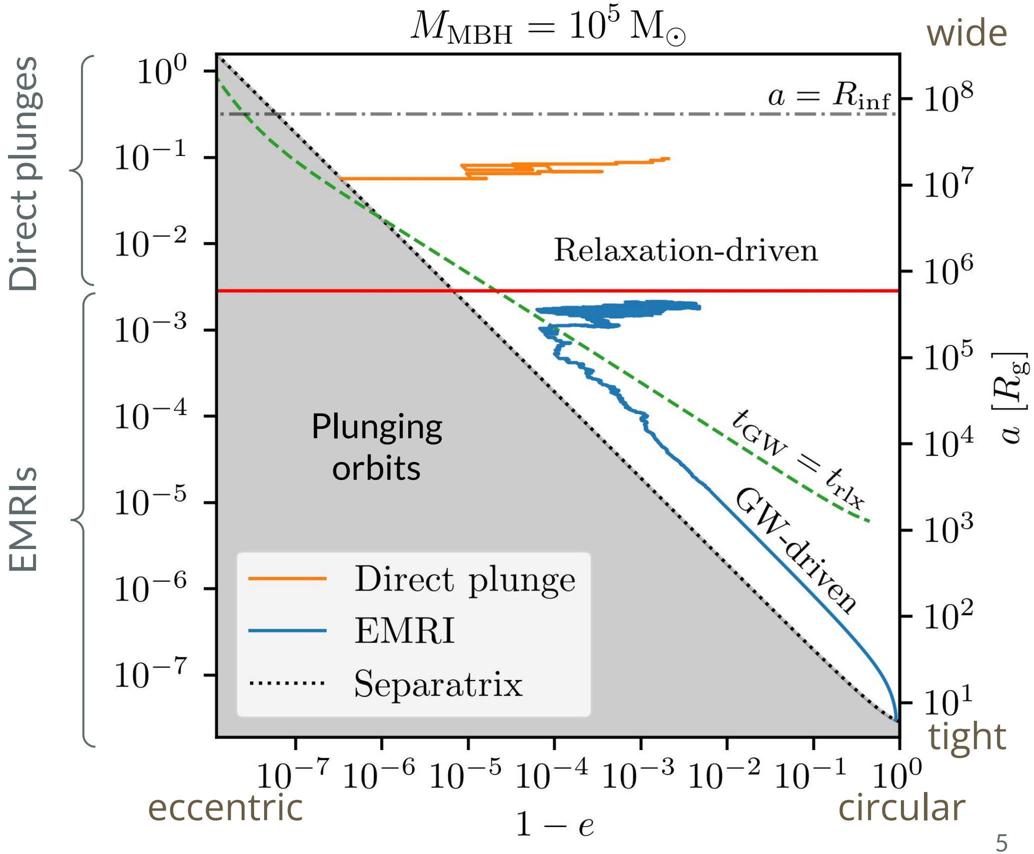

Cliffhanger EMRIs

First observed in simulations by Qunbar&Stone24

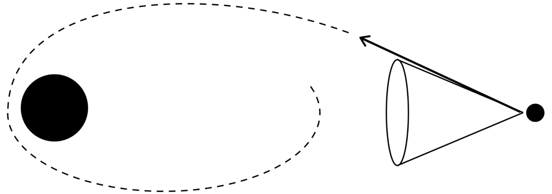

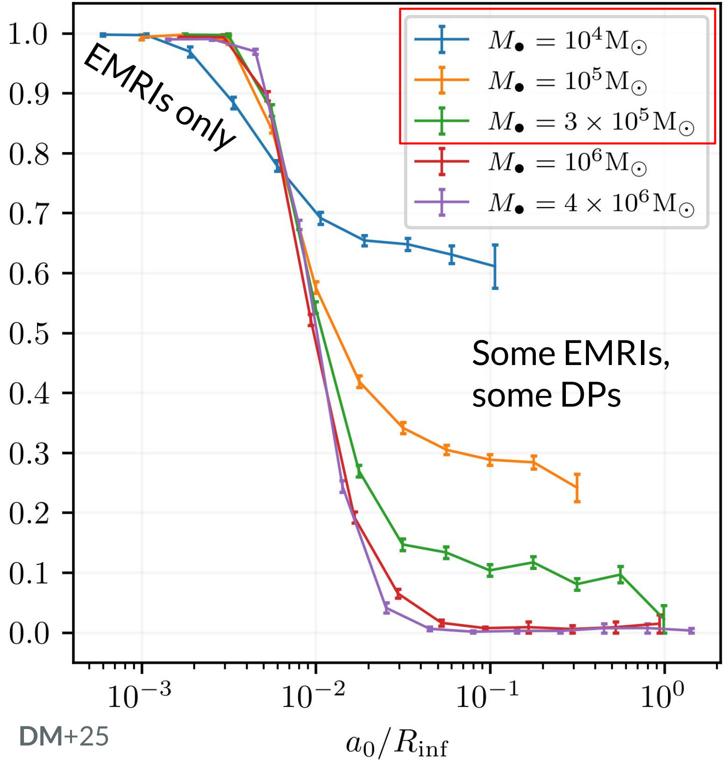

DM+25

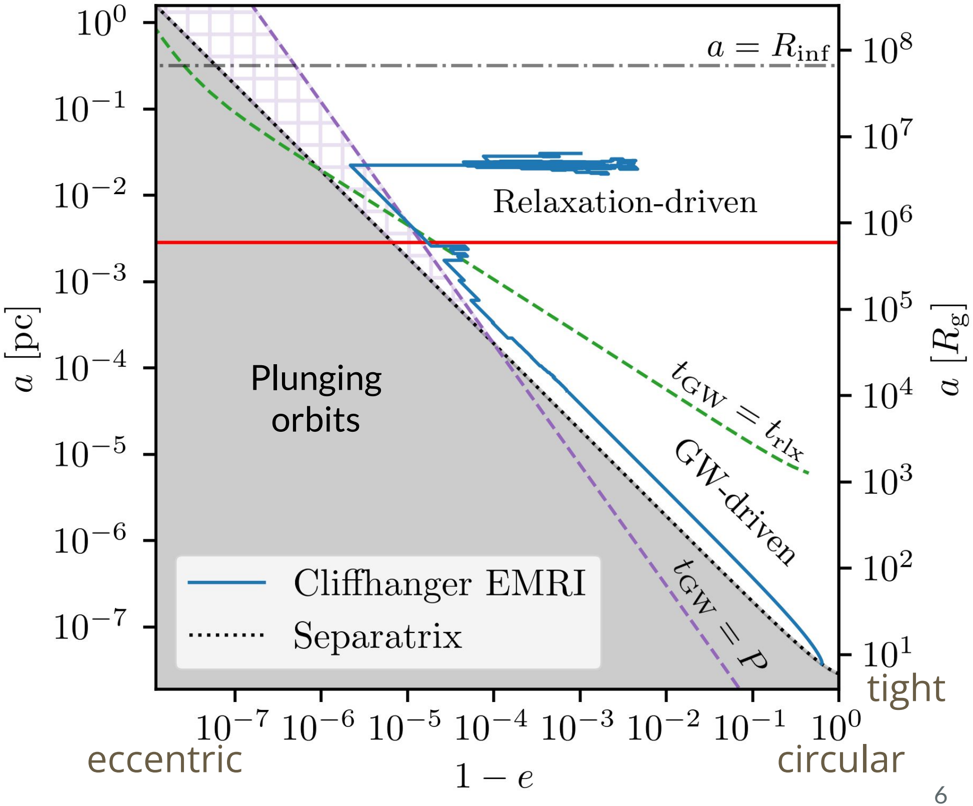

Integration steps

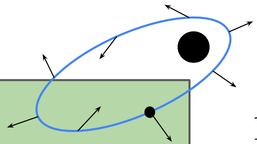

DM+25

Monte Carlo

- Timestep much smaller than a period
- Local treatment of two-body relaxation
- 2.5PN (post-Newtonian) dynamics

DM+26

FastEMRIWaveforms (Chapman-Bird+25)

- Large timesteps initially; short near the end
- No relaxation (ok during the inspiral)
- Accurate dynamics in strong-field:
  - 5PN analytical fluxes
  - Numerical fluxes from Teukolsky eq. (for e < 0.9)

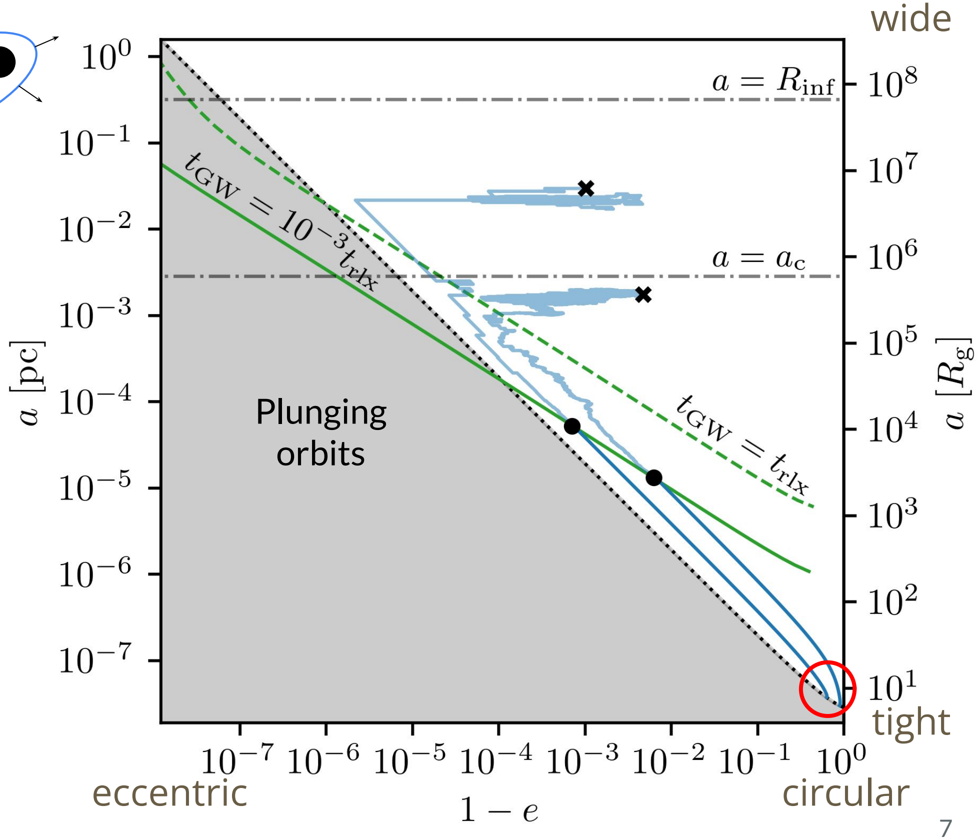

Astrophysical weighting

Weight each run by the rate of EMRIs forming at that initial semi-major axis (from Fokker-Planck evolution of the cluster, Broggi+22)

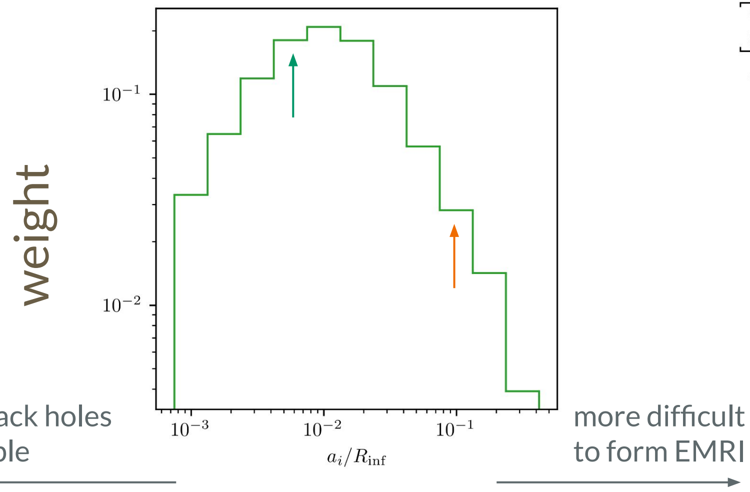

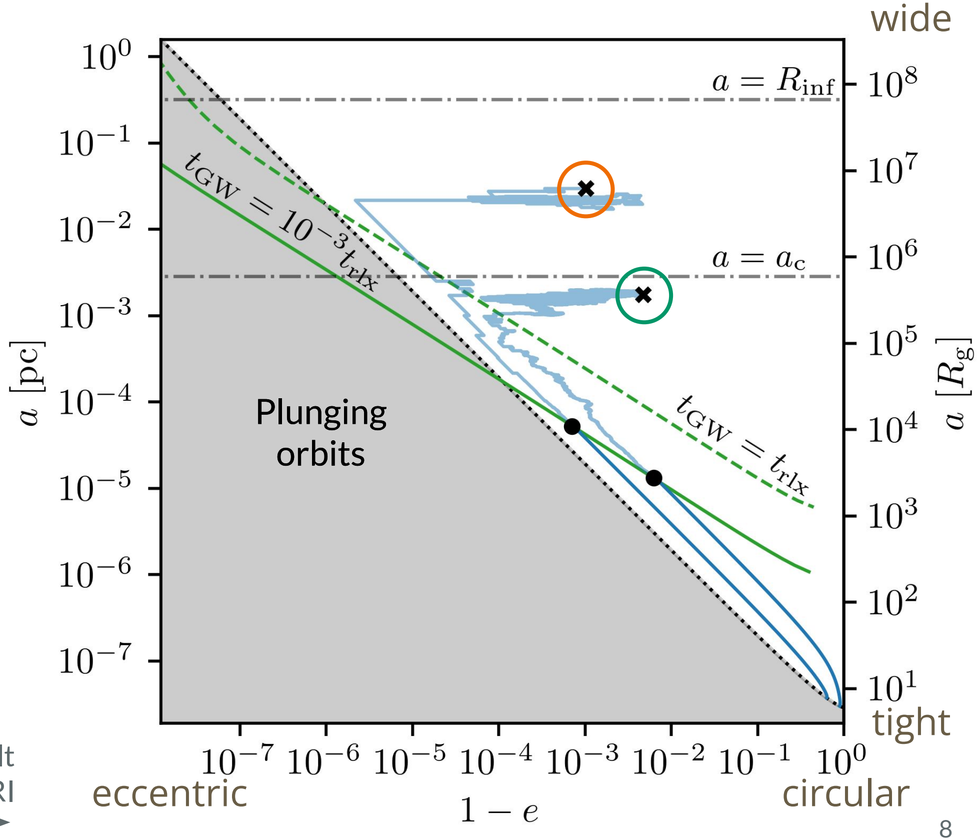

Eccentricity distribution

- Peak at e = 0.2 and large fraction of EMRIs at larger eccentricities
- Cliffhanger EMRIs dominate at large eccentricity, but classical EMRI can be highly eccentric as well

Fraction outside FEW's accurate range (e > 0.9):

time	$10^5\,\mathrm{M}_\odot$	$3\times10^5\,\mathrm{M}_\odot$	$10^6\,\mathrm{M}_\odot$	$4\times10^6\,\mathrm{M}_\odot$
2 years	75.4 %	38.9 %	5.3 %	0.6 %
1 year	65.0 %	27.8 %	2.9 %	0.5 %
6 months	52.5 %	18.0 %	1.6 %	0.4 %
3 months	42.0 %	11.0 %	0.9 %	0.4 %

(more MBH masses in the paper)

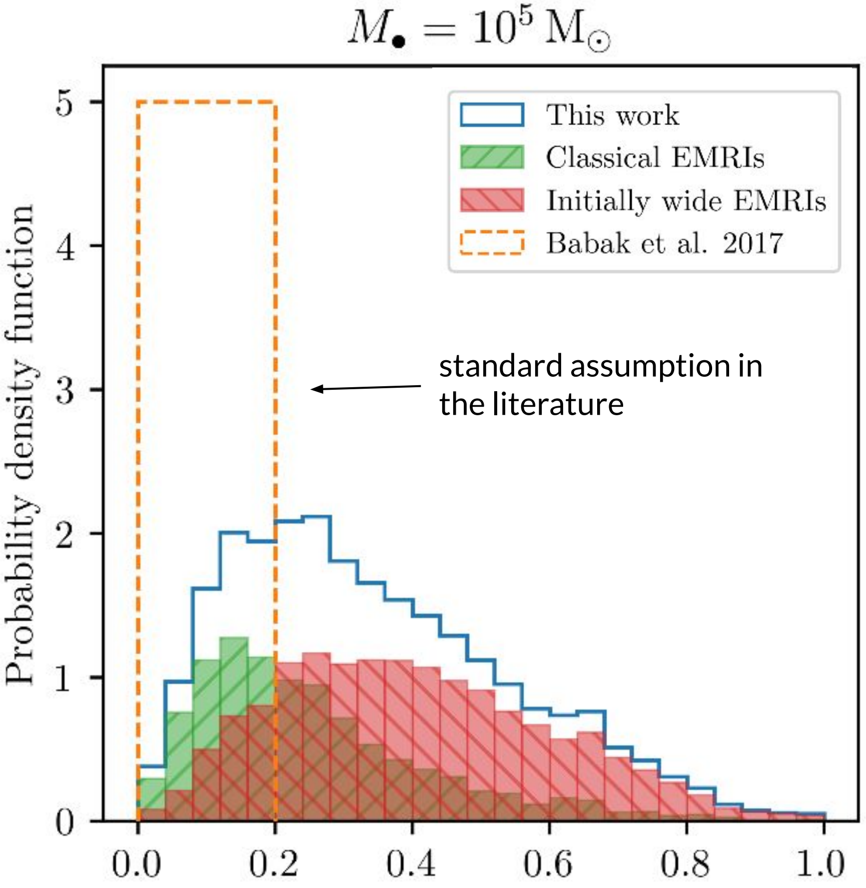

eccentricity at merger

DM+26

The Hills mechanism

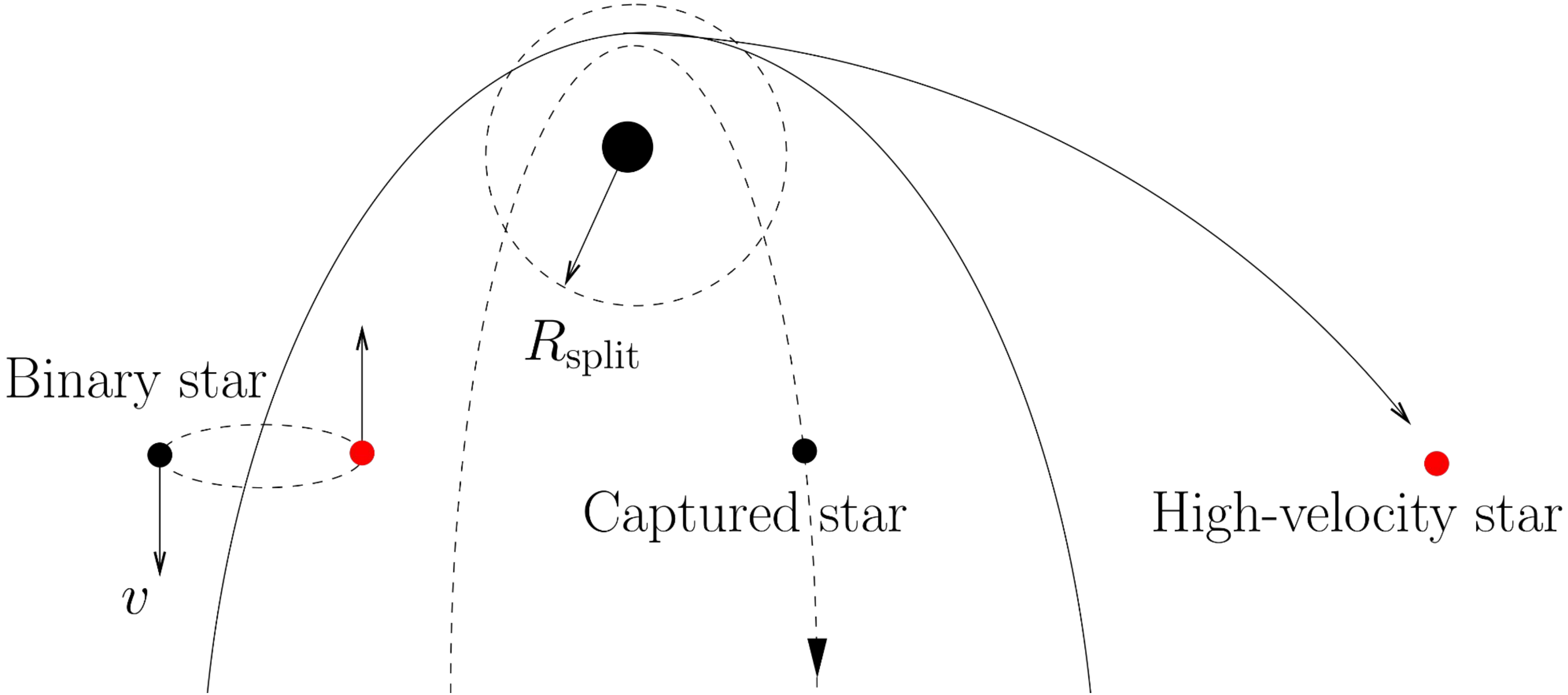

Amaro-Seoane18

Methods

PRELIMINARY

Rate and properties of binaries passing close to the MBH

↓

Tidally-break binaries

↓

Relaxation acting on deposited single black holes — Monte Carlo

↓

Inspiral to final plunge — FEW

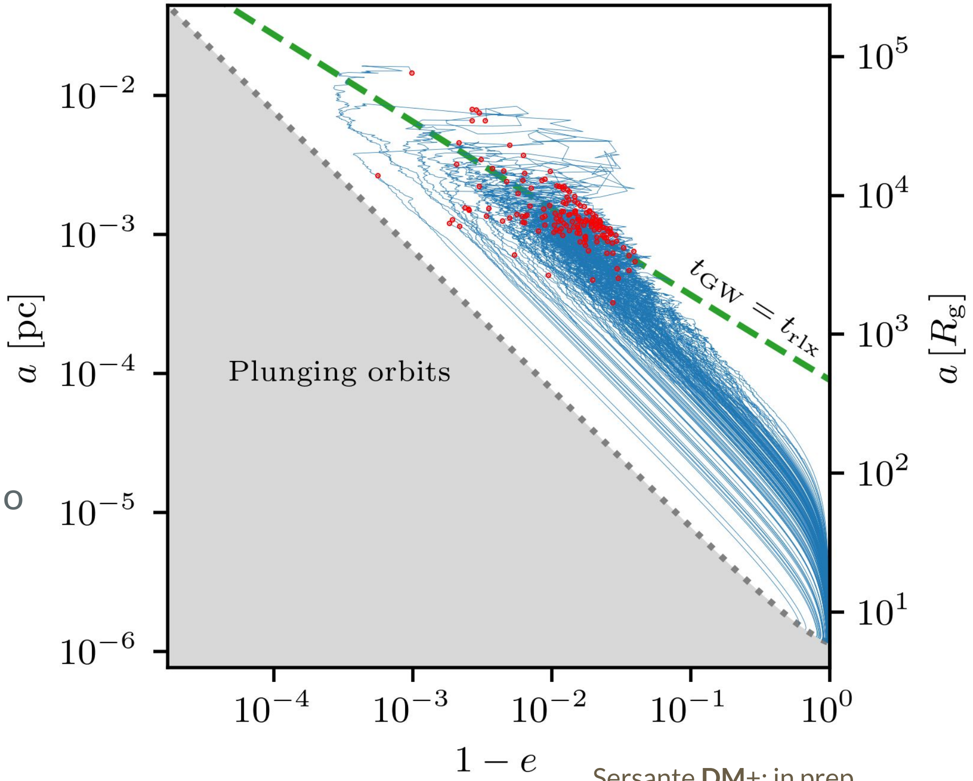

Sersante,**DM**+; in prep.

Methods

Rate and properties of binaries passing close to the MBH

Tidally-break binaries

Relaxation acting on deposited single black holes

Inspiral to final plunge

Fokker-Planck solver for the cluster

Restricted three-body integrator

PRELIMINARY

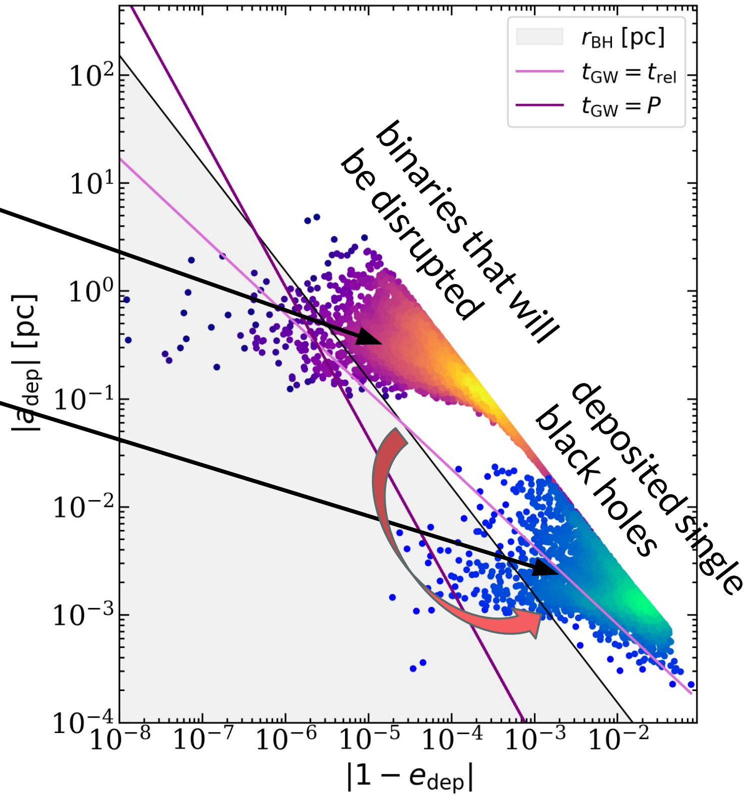

Sersante,**DM**+; in prep.

Eccentricity distribution

(Note) Relaxation: single black holes only; Hills: binary black holes only. Unrealistic!!

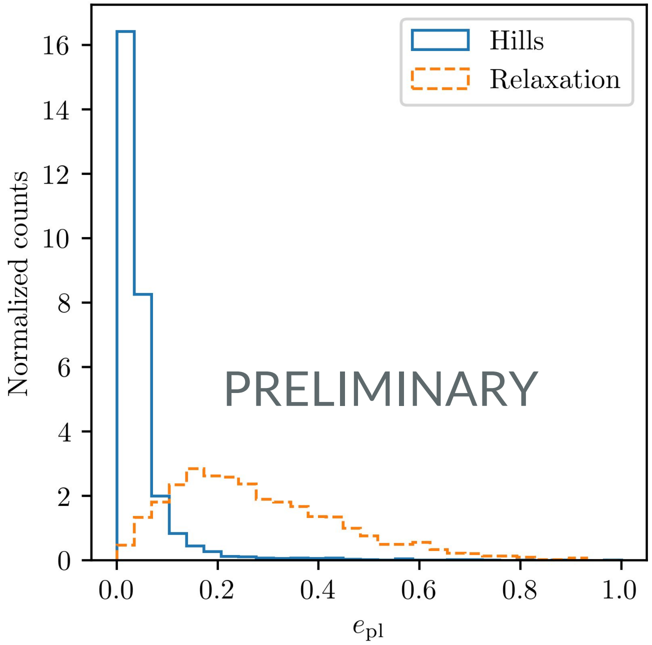

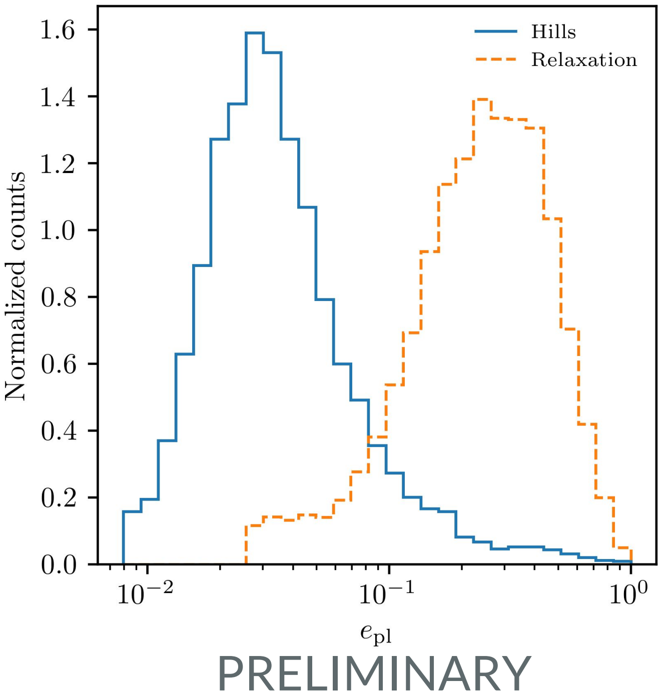

Relaxation:
peaks at 0.2-0.3

Hills:
peaks at 0.02-0.03

Sersante,**DM**+; in prep.

Summary

- Cliffhanger EMRIs break the classical EMRI / direct plunge picture: EMRIs can originate from initially wide orbits around MBHs with masses below $10^6\ M_\odot$
- Two-body relaxation EMRIs are substantially more eccentric than previously expected (peak at $e = 0.2–0.3$)
- Fast EMRI waveform models may miss a significant fraction of these systems unless they are extended to larger eccentricities
- Hills EMRIs remain much more circular (peak at $e = 0.02–0.03$), providing a potential observational discriminant between formation channels

Extra slides

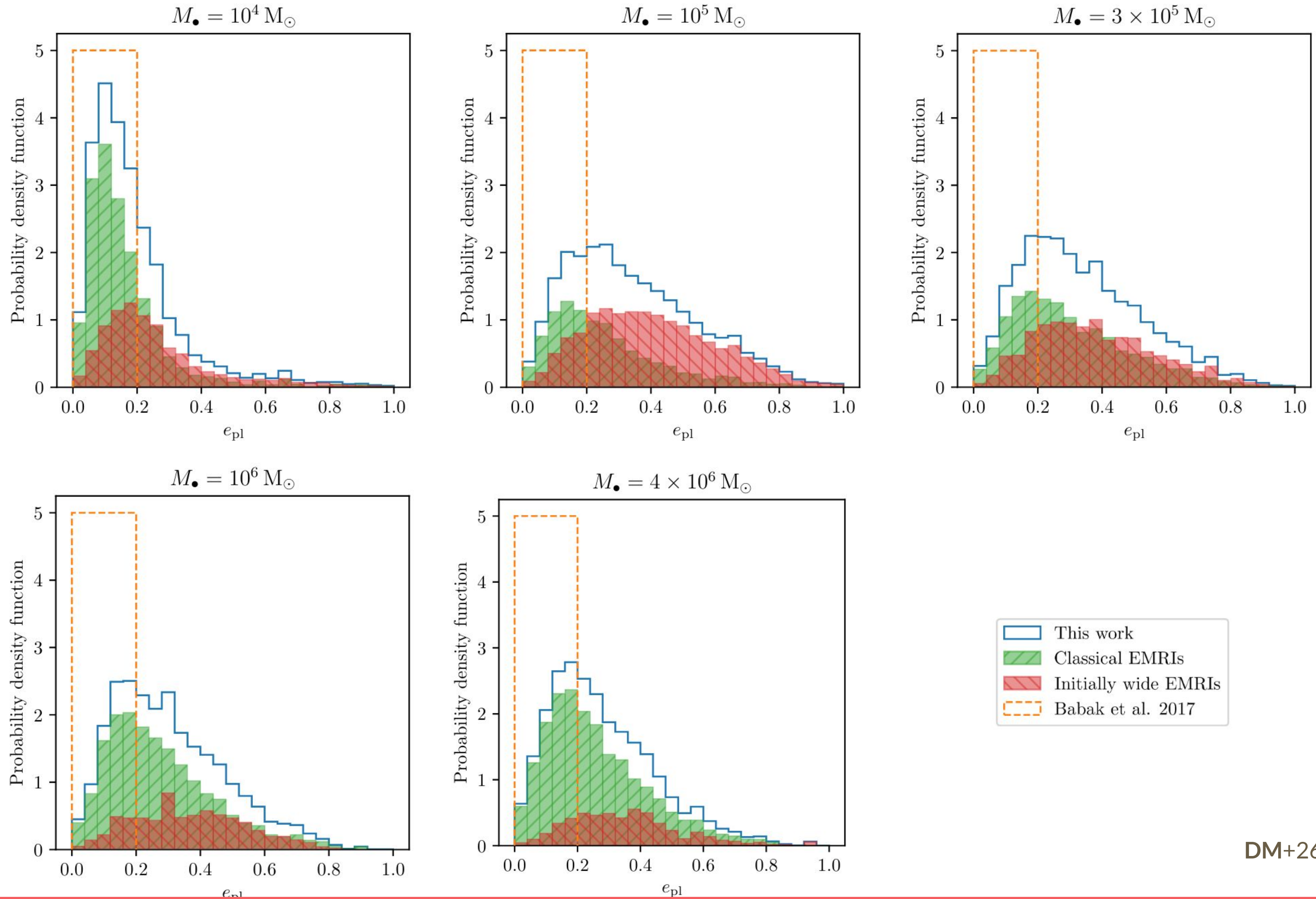
$M_\bullet = 10^4\,\mathrm{M}_\odot$
$M_\bullet = 10^5\,\mathrm{M}_\odot$
$M_\bullet = 3 \times 10^5\,\mathrm{M}_\odot$
$M_\bullet = 10^6\,\mathrm{M}_\odot$
$M_\bullet = 4 \times 10^6\,\mathrm{M}_\odot$
Probability density function
e_{pl}
This work
Classical EMRIs
Initially wide EMRIs
Babak et al. 2017

DM+26

Issues for detection

Fraction of the population outside FEW's range (e > 0.9):

time	$10^5\,M_\odot$	$3\times10^5\,M_\odot$	$10^6\,M_\odot$	$4\times10^6\,M_\odot$
2 years	75.4 %	38.9 %	5.3 %	0.6 %
1 year	65.0 %	27.8 %	2.9 %	0.5 %
6 months	52.5 %	18.0 %	1.6 %	0.4 %
3 months	42.0 %	11.0 %	0.9 %	0.4 %

Must extend fast waveform models at higher eccentricities

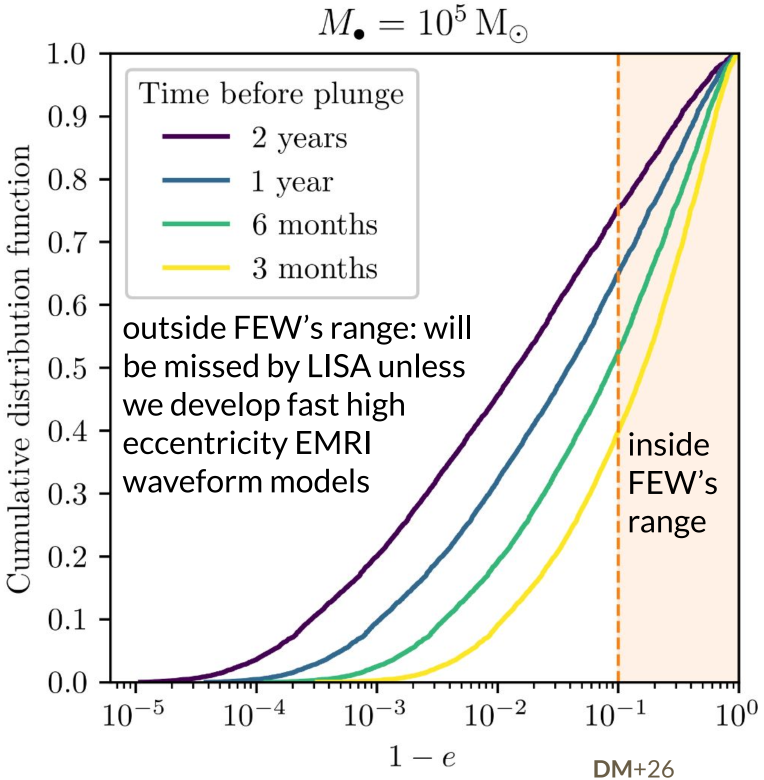

DM+26

Cliffhanger EMRIs

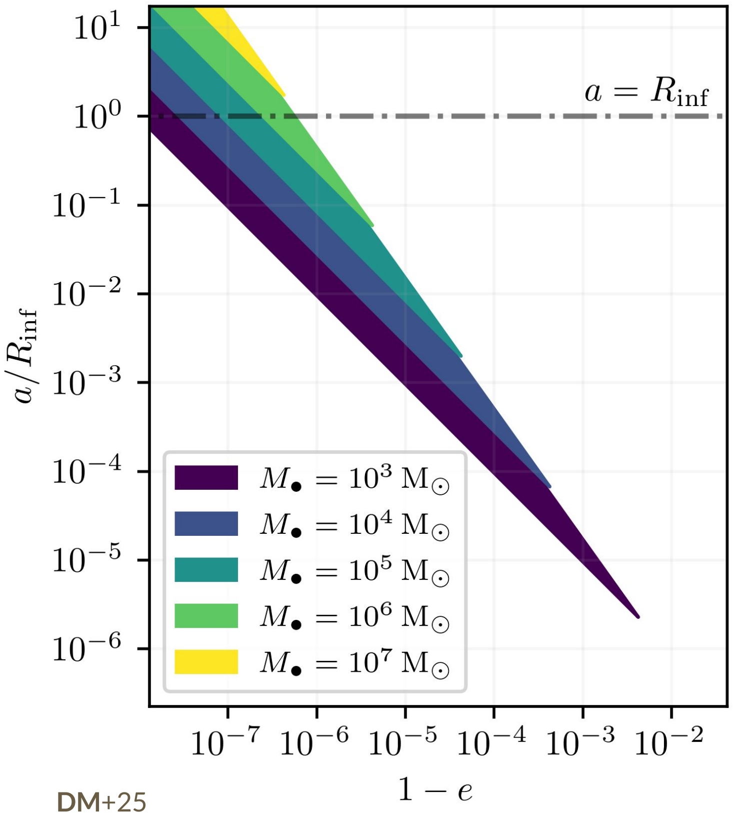

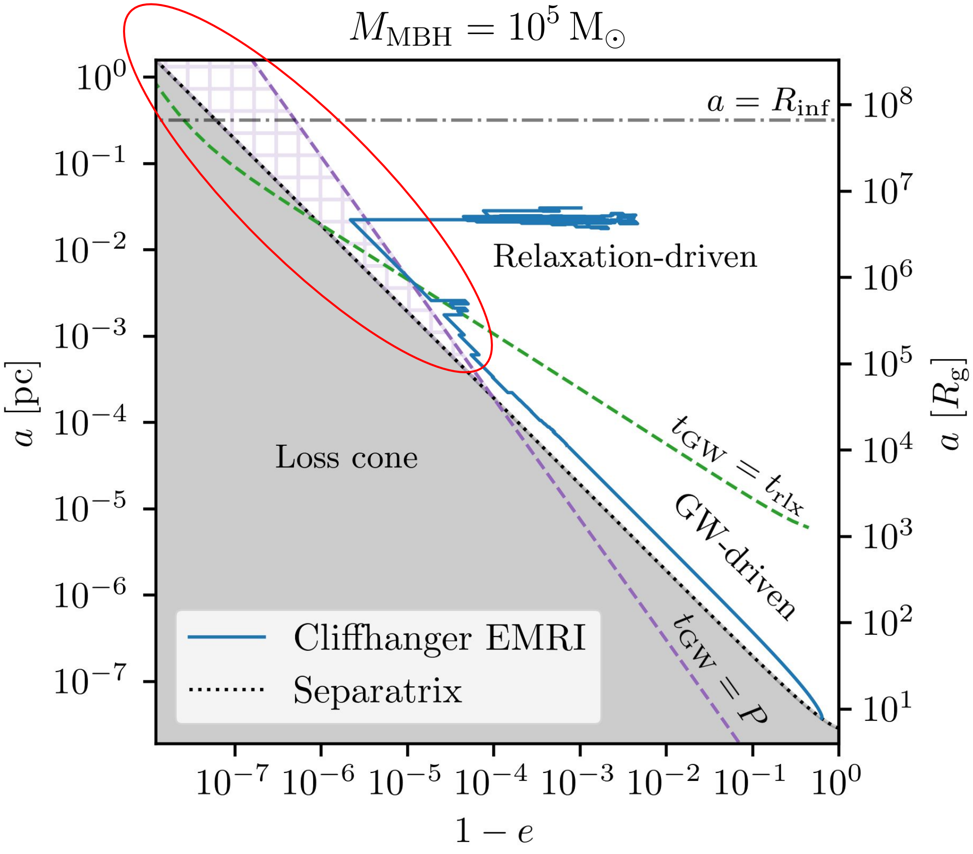

DM+25

Rates

Table 1. Instantaneous EMRI+DP ($\dot{N}$), EMRI ($\dot{N}_{\rm EMRI}$), and DP ($\dot{N}_{\rm DP}$) rates produced in the snapshots we investigated.

$M_\bullet$ [M$_\odot$]	t [Myr]	$\dot{N}$ [yr^{-1}]	$\dot{N}^{\rm cl}_{\rm EMRI}$ [yr^{-1}]	$\dot{N}_{\rm EMRI}$ [yr^{-1}]	$\dot{N}^{\rm cl}_{\rm DP}$ [yr^{-1}]	$\dot{N}_{\rm DP}$ [yr^{-1}]
10^4	0.58	5.9×10^{-7}	5.3×10^{-7}	4.0×10^{-7}	6.5×10^{-8}	1.9×10^{-7}
10^5	11	6.6×10^{-7}	3.1×10^{-7}	2.9×10^{-7}	3.7×10^{-7}	3.8×10^{-7}
3×10^5	25	3.5×10^{-7}	4.9×10^{-8}	6.7×10^{-8}	3.0×10^{-7}	2.8×10^{-7}
3×10^5	45	7.4×10^{-7}	2.0×10^{-7}	2.1×10^{-7}	5.4×10^{-7}	5.3×10^{-7}

Notes. We report estimates according to our formulation Eq. (62) (no superscript) based on the transfer function $S(a_0)$, and the classical estimates Eq. (64) (superscript cl) based solely on the critical semi-major axis $a_c = 0.01\,R_{\rm inf}$.

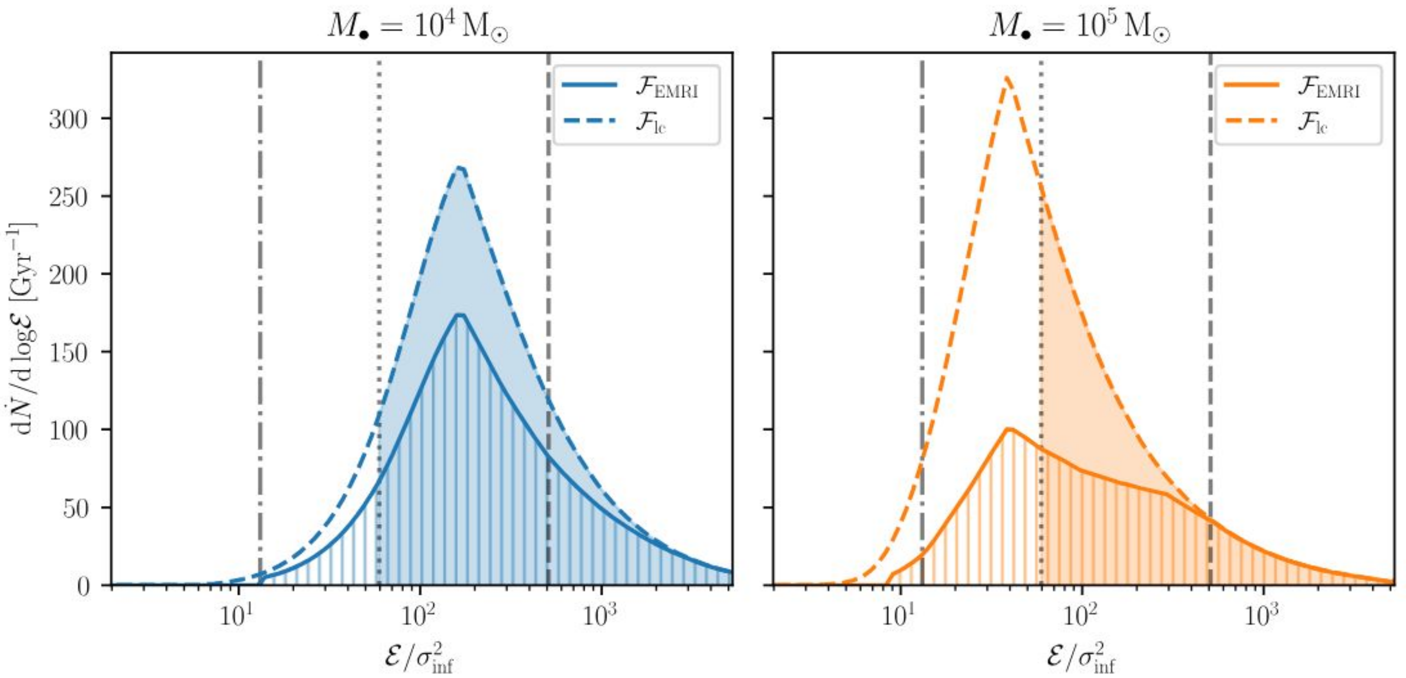

DM+25

Formation channels for EMRIs

Stellar-dynamical processes in dense nuclear star cluster
(e.g. Hopman&Alexander05, Miller+05, Bar-Or&Alexander16, Broggi+22, Kaur+24, Zhang&Amaro-Seoane24)

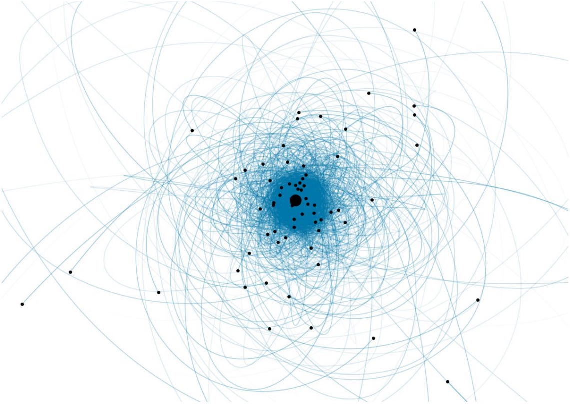

Gas-assisted capture and inspiral in AGN accretion disks
(e.g. Levin07, Pan&Yang21, Derdzinski&Mayer23)

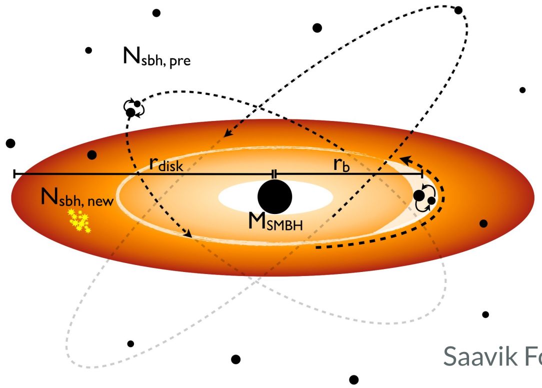

Saavik Ford+19

+ others...

Methodology improvements

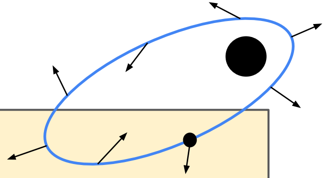

Qunbar&Stone24
- Newtonian dynamics
- Two-body relaxation is orbit-averaged

DM+25
- 2.5 **post-Newtonian** dynamics
- Two-body relaxation is **local**

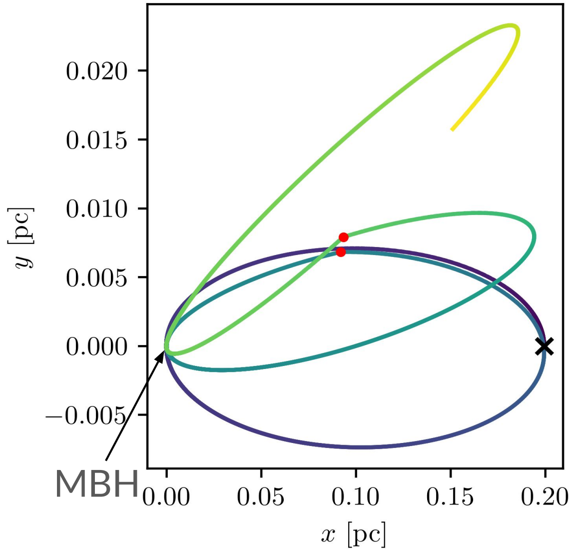

$$\epsilon \sim (v/c)^2$$

$$\frac{d\mathbf{v}}{dt} = \frac{Gm}{r^2}\left\{-\hat{\mathbf{n}} + \frac{1}{c^2}\mathbf{A}_{1PN} + \frac{1}{c^4}\mathbf{A}_{2PN} + \frac{1}{c^5}\mathbf{A}_{2.5PN}\right.$$

Not N-body!
Both are Monte Carlo approaches

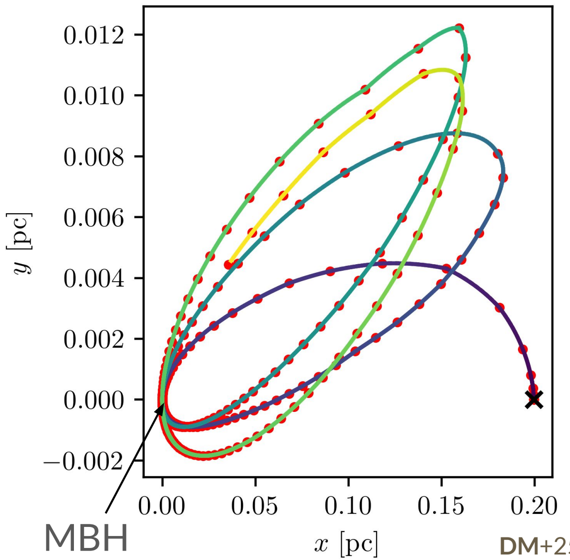

DM+25

Astrophysical weighting

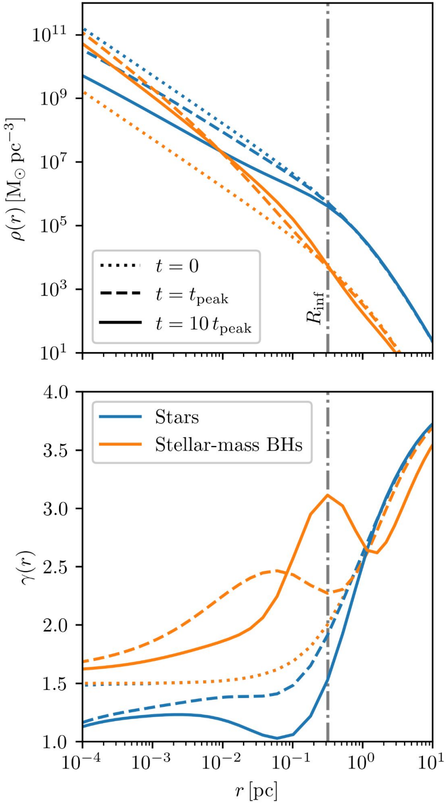

- The nuclear star cluster is evolved with a Fokker-Planck solver (Broggi+22)
- The EMRI production rate evolves with time
- The time-averaged differential rate is used to weight runs

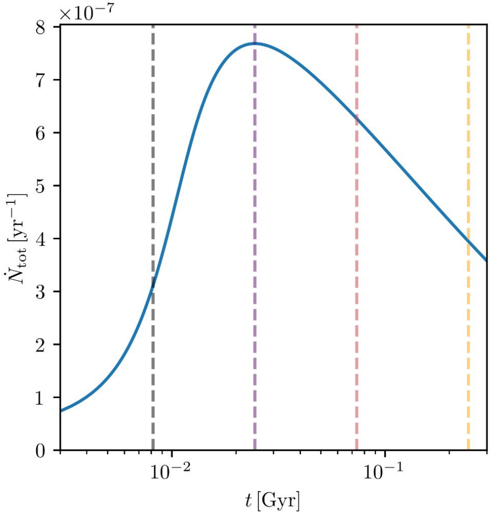

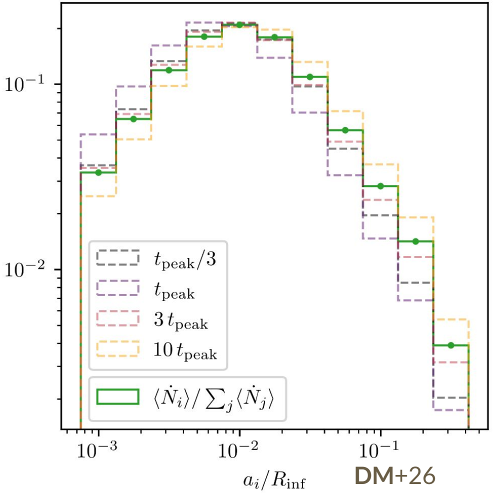

DM+26